DOI: 10.21062/mft.2021.013 http://www.journalmt.com

Corrosion Resistance of Ferritic Stainless Steel X12Cr13 After Application of Low-Temperature and High-Temperature Plasma Nitriding

David Kusmič[1], Ondřej Čech[2], Lenka Klakurková[3]
[1]University of Defence, Department of Mechanical Engineering, Kounicova 65, 602 00 Brno, Czech Republic, EU, david.kusmic@unob.cz
[2]Brno University of Technology, Department of Electrical and Electronic Technology, Technická 3058/10, 616 00 Brno, Czech Republic, EU, cechondrej@feec.vutbr.cz
[3]CEITEC Brno University of Technology, Research Group RG 1-06, Brno, Czech Republic, EU, lenka.klakurkova@ceitec.vutbr.cz

The impact of plasma nitriding process on corrosion resistance of ferrettic stainless steel (FSS) was evaluated in this study. The FSS X12Cr13 (AISI 410) was subjected to low-temperature plasma nitriding (LTPN) treatment at a temperature of 400°C in $3H_2$:$1N_2$ (l/h) and in $1H_2$:$3N_2$ (l/h) reverse working atmosphere (LTPN-R) and to high-temperature plasma nitriding (HTPN) treatment at 550 °C for 15 h. The microstructure and microhardness of the untreated and nitrided stainless steel were evaluated. The corrosion properties of the untreated and plasma nitrided steel samples were evaluated using the anodic potentiodynamic polarization tests in neutral 2.5% NaCl deaerated solution. The phase analysis showed that LTPN and LTPN-R treatment on the AISI 410 steel led to the formation of α_N layer (nitrogen expanded ferrite) accompanied by Fe_3C and Fe_4N iron nitrides and CrN. The HTPN technique led additionally to the formation of an increased volume of Cr_4N_4 chromium nitrides and $Cr_{15}Fe_7C_6$ chromium iron carbide. The plasma nitriding process significantly increased the microhardness of the ferritic stainless steel. The pitting was evaluated, and the pitting coefficient was calculated. The electrochemical corrosion tests showed the best corrosion resistance of the untreated X12Cr13 stainless steel, only slightly increased corrosion rates of LTPN and LTPN-R techniques, and extreme corrosion rates after application of the HTPN technique, causing Cr depletion and thereby suppressing the ability to passivation.

Keywords: plasma nitriding, ferritic stainless steel, corrosion resistance

1 Introduction

One of the processes of surface treatment based on chemical-heat treatment is the plasma nitriding (PN) process. This PN process is mainly used to improve the mechanical properties such as surface hardness, fatigue strength [1, 2], and tribological properties [3, 4] of structural steels. On the other hand, some of the mechanical properties, for example, notch toughness, are reduced by the plasma nitriding process [5]. Plasma nitriding of structural carbon steels is typically carried out in the range of 450 ÷ 550 °C and is mostly limited by previous heat treatment temperatures [1, 2] The increase of corrosion resistance may occur under certain conditions after plasma nitriding in the case of structural carbon steels [6].

The aim of the improvement of the mechanical properties of plasma nitrided stainless steels is similar to the required improvement of mechanical properties of plasma nitrided structural carbon steels. However, most studies related to nitriding of stainless steel have mostly dealt with austenitic stainless or martensitic steels, but very few have focused on ferritic stainless steel (FSS). For example, the surface hardness of FSS AISI 410 stainless steel is increased rapidly after 20 h of plasma nitriding at 400 °C and in nitriding atmosphere $1H_2$:$3N_2$ (l/h), up to 1275 HV [3]. The corrosion resistance of stainless steel is directly dependent on plasma nitriding parameters as the time duration of the process, composition of nitriding (working) atmosphere, and especially the temperature of the PN process. The corrosion resistance is strongly on phase composition dependent. Especially to CrN precipitation over 723 K (450 °C), related to the decomposition of α_N or S^α phase (supersaturated solid solution of nitrogen in the ferritic phase) to $\alpha_N \rightarrow$ CrN and Cr depletion [8]. The authors state, that the corrosion resistance of stainless steels can be impaired if the process of plasma nitriding is carried out at temperatures 450 - 480 °C [9], 460 °C for AISI 304 stainless steel [10], 475 °C [11], and 480 °C [12]. For example, plasma nitrided AISI 410 steel at temperature 420 °C for 6 hours obtained better corrosion resistance than the un-nitrided one [13], as similar to X12CrMoWVNbN10-1-1 martensitic stainless steel [14]. On the other hand, the FSS (AISI 410) plasma

nitrided at temperature 500 °C had been affected by decreased corrosion resistance, as expected [15].

It is stated that above the threshold of 450 - 480 °C (depends on the type of steel) the precipitation of iron and chromium nitrides (CrN) on the grain boundaries in the nitriding affected layer occurs [10]. At PN temperature of 500 °C, the nitride layer consists of CrN, Fe_3N, and Fe_4N phases for AISI 304 steel, and the pitting corrosion was observed [10]. Similar behavior was observed at 500 °C for plasma nitrided AISI 410 stainless steel as well [15].

2 Experimental

The FSS X12Cr13 was used in the form of sheets with the original size of 150 x 80 x 1 mm. The original sheets were used for verification of chemical composition and X-ray phase analysis of untreated and later of PN treated steel samples. Chemical composition has been verified using the spectrometer Tasman Q4 (in wt.%): 0.002 C, 0.37 Si, 1.33 Mn, 0.079 P, 0.0005 S, 11.6 Cr, 0.54 Ni, and compared to the inspection certificate

For potentiodynamic polarization testing (PPT) were the original steel plates cut and rounded to experimental samples with a diameter of 15 mm, needed for the internal diameter of the potentiostat sample holder (without additional polishing the surface). Both types of experimental samples were degreased in ethanol before the PN process and before every measurement. Prepared samples were subjected to the PN process in the RUBIG PN 60/60 device. Plasma cleaning, nitriding parameters, and sample marking are listed in Tab. 1.

Tab. 1 *Plasma nitriding parameters and sample marking*

Samples	Temperature (°C)	Duration (h)	Bias (V)	Pressure (Pa)	Gas ratio (l/h)
untreated	-	-	-	-	-
Plasma cleaning	380	1	700	80	$20H_2$:$2N_2$
LTPN	400	15	520	280	$24H_2$:$8N_2$
LTPN-R	400	15	520	280	$8H_2$:$24N_2$
HTPN	550	15	520	280	$24H_2$:$8N_2$

Structures of plasma nitrided experimental samples were documented using the Scanning Electron Microscopy – Back Scattered Electron (SEM-BSE). Thanks to etching by 2% Nital the nitrogen modified surface layers morphology were observed as can be seen in Fig. 1 for LTPN, in Fig. 2 for LTPN-R and Fig. 3 for HTPN technique.

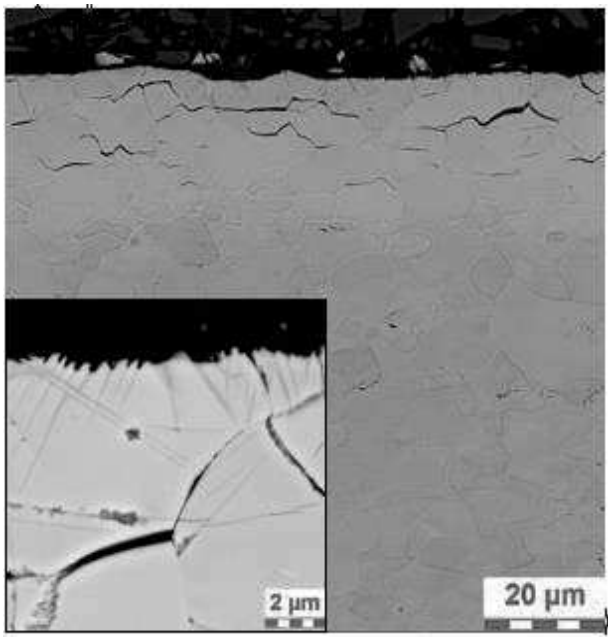

Fig. 1 *Microstructures of LTPN treated X12Cr13 steel, etching sensitive grain boundaries*

The PN led to the formation of deformed α_N nitrogen expanded ferritic grains in the close surface layer [16]. The deformation of expanded ferritic grains induced the formation of deformation bands, aligned at 45° to the surface (Fig. 1 and Fig. 2) [16]. Intergranular cracking occurs after LTPN, LTPN-R, and HTPN techniques in the nitrogen affected zone (α_N layer) as seen in Figures 1 – 3. The intergranular cracking is attributed to elevated internal compressive stress in the α_N layer. Additionally, the PN conditions led to increased sensitivity to etching along the grain boundaries related to FexN iron nitrides formation and precipitation of CrN, as documented X-ray phase analyses in Fig. 5.

The nitrogen affected zone (α_N layer) was approximately in the range of 12 ± 3 µm for LTPN and 49 ± 2 µm for LTPN-R according to light-microscopy measurement (LM), as summarized in Tab. 2. The HTPN technique created an extensive affected zone (70 ± 3 µm) with intensive FexN and CrN precipitation (Fig. 3), and additionally Cr_4N_4 and $Cr_{15}Fe_7C_6$ chromium nitrides precipitated (simplified as CrxN), as later analyzed in Fig. 5. Contrary, the morphology of HTPN FSS AISI 410 is different from low-temperature PN techniques. Deformation bands were not documented in the close surface layer. The HTPN condition led to the formation of intergranular cracking too and to the intergranular eutectoid microstructure in the nitrogen affected grains, as do-

cumented in Fig. 3. Some authors documented a lamellar eutectoid (α + CrN) [17], [18]. Nevertheless, the eutectoid lamellar structure (α + CrN) wasn´t documented in this study.

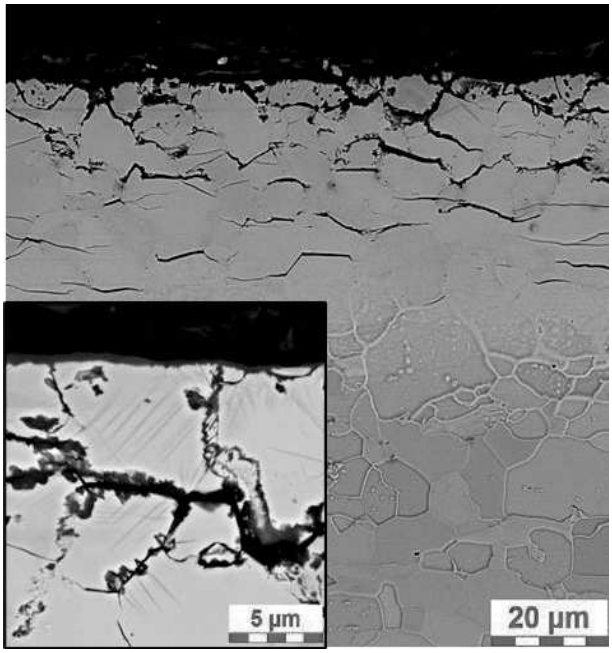

Fig. 2 *Microstructures of LTPN-R treated X12Cr13 steel, etching sensitive grain boundaries*

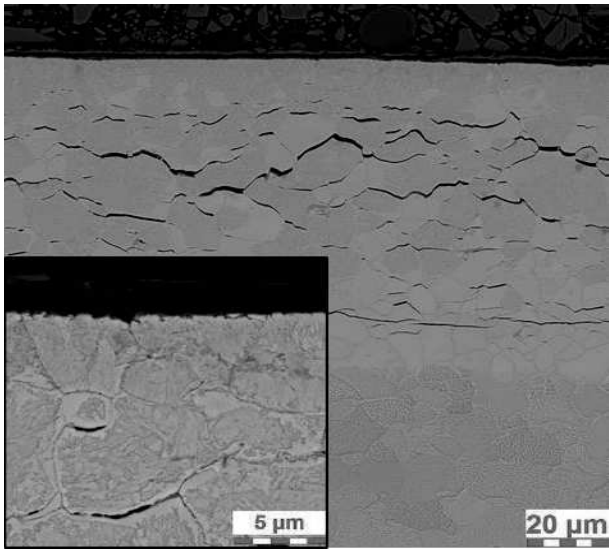

Fig. 3 *Microstructures of LTPN, LTPN-R, and HTPN treated X12Cr13 steel*

After PN was the microhardness and the microhardness profile measured using the microhardness tester Leco LM247 AT, according to ISO 18203:2016 standard on prepared cross-sectional samples. Microhardness testing was performed using the Vickers indenter, the load was 0.49 N, dwell time at load was 12 s and the NHD value (Nitriding Hardness Depth) was determined.

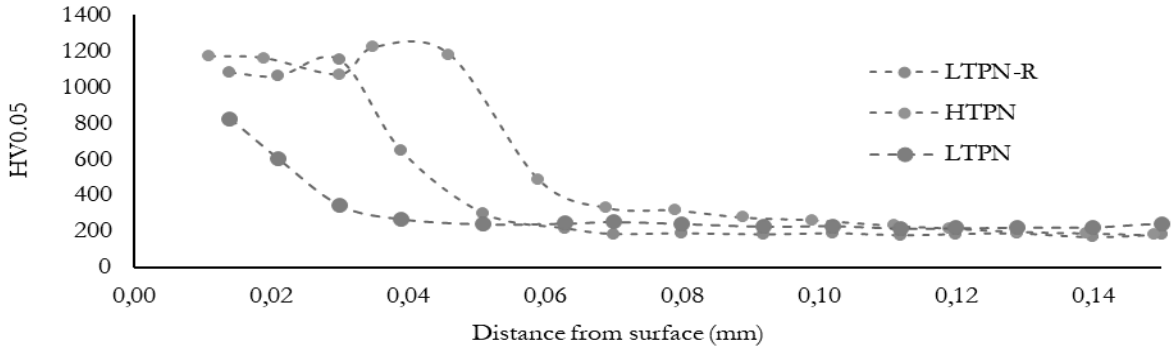

Fig. 4 *Microhardness measuring of treated X12Cr13 steel (Leco LM247 AT)*

The microhardness profile was measured at 3 locations on each sample and finally averaged, so the measuring of nitride layer depth was accomplished and plotted in Fig. 4 and summarized in Tab. 2. The LTPN and LTPN-R technique increased microhardness, compared to untreated steel (180 – 255 HV0.05). The maximal values of microhardness reached 911 ± 12 HV0.05 for LTPN and 1047 ± 21 HV0.05 for the LTPN-R technique. Increased microhardness after LTPN and LTPN-R is related to elevated internal compressive stress in the formed α_N layer and to the presence of γ'-Fe_4N, ε-$Fe_{2-3}N$ (Fe_xN) [15, 16]. The highest microhardness reached the HTPN treatment (1193 ± 22 HV), related to an increased volume of γ'-Fe_4N and CrN (Fig. 5) [16].

Tab. 2 *Surface hardness, microhardness, depth of γN layer obtained under different PN conditions*

Samples	Layer depth measured by LM (µm)	Microhardness testing HV0.05	
		NHD (µm)	Microhardness
untreated	-	-	180 - 255
LTPN	12 ± 3	39	911 ± 12
LTPN-R	49 ± 2	57	1047 ± 21
HTPN	70 ± 3	112	1193 ± 22

As seen, the nitrogen affected zone (α_N layer) of the LTPN-R technique is thicker according to LM measurement and NHD compared to the LTPN technique thanks to the increased ratio of H_2 in the working atmosphere. The greatest NHD value and thickness measured by LM of α_N layer has been documented for HTPN treatment (Fig. 4 and 2, Tab. 2).

It is evident, that the LM measuring doesn´t meet the NHD values, generally for all PN treatments (Tab. 2.). Measured NHD values are higher than the measured α_N layer thickness by LM. This phenomenon is most likely related to the nitrogen/carbon competition during PN leading to the creation of a limited α_C zone (supersaturated solid solution of carbon in the ferritic phase) beneath the nitrogen modified layer (α_N + FexN + CrxN). This α_C zone is characterized by internal compressive stresses, which increases additionally the microhardness (shifting of NHD to higher values). Some authors revealed an accumulated carbon layer beyond the nitrogen plateau on the nitrided or nitrocarburized austenitic stainless steels, as documented by glow-discharge optical emission spectroscopy (GDOES) concentration profiles [19]. This phenomenon was not deeply investigated in this research.

The X-ray phase analysis was performed by XRD Rigaku Miniflex 600 device (Rigaku D/teX Ultra 250, Cu Kα radiation), using PDXL software with PDF-2 and Crystallographic Open Database for the quantitative analysis. Results of phase analysis for untreated, LTPN, LTPN-R, and HTPN treated FSS AISI 410 are summarized in Fig. 5. A shift of α_N peaks to lower angel compared to the original α-Fe peak, can be seen on the plotted diffraction peaks for all PN treatments (Fig. 5). Nevertheless, the diffraction peaks proving the existence of α_C are not detected. There can be seen visible peaks of iron nitrides ε-$Fe_{2-3}N$ (simplified as Fe_3N) and γ-Fe_4N nitrides and even the CrN was detected for all types of PN processes. Additionally, the Cr_4N_4 and $Cr_{15}Fe_7C_6$ chromium nitrides (simplified as CrN) were certainly analyzed in the nitrogen affected zone after HTPN treatment (Fig. 5). It is clear that even so LTPN and LTPN-R treatment conditions let to the formation of CrN, which are responsible for the deterioration of corrosion properties of PN treated stainless steels.

Anodic PTT was carried out on untreated and PN treated X12Cr13 steel samples. The potentiostat Biologic SP 150 as the main measuring device with software EC-Lab V11.10. was used for calculating values of corrosion

characteristics. The Cyclic Potentiodynamic Polarization method (ASTM-61) was chosen as a method for measuring chosen corrosion characteristics. The parameters of this method were the following: sweep speed dE/dt = 0.166 mV/s, Ei = -0.25 V, EL = 2 V, Ip = 25 mA, E range (-2 V;2 V) at ambient temperature in neutral deaerated 2.5% NaCl solution. The measured surface of steel samples was 0.865 cm².

Anodic potentiodynamic measurement involves polarizing the working electrode (sample) from its equilibrium potential Eoc (OCP – open circuit potential), by steadily shifting the DC potential difference between the working electrode and the counter electrode (SCE) by the potentiostat, while recording the current response (see Fig. 6).

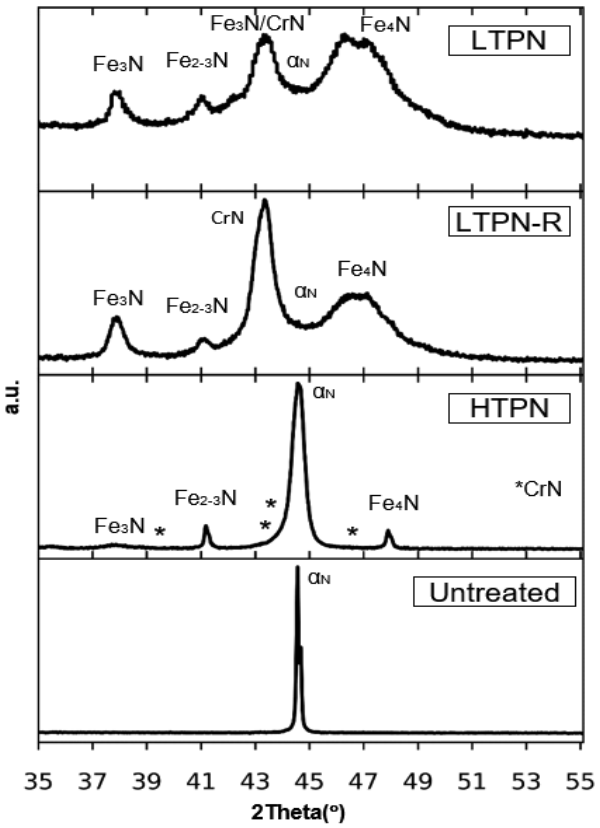

Fig. 5 *Phase analysis of PN treated and untreated X12Cr13 steel*

The Tafels constants βa and βc were determined from the anodic and cathodic branch of the polarization curves, as well as the Corrosion potential Ecorr (mV) and Total anodic current Icorr (μA) values. Using the software EC-Lab V11.10 were further the values of Polarization resistance Rp (Ohm) and values of Corrosion rates calculated. All calculations represent the average values of three measurements are summarized in Tab. 3.

Surfaces of plasma nitrided and untreated samples were additionally documented by the light microscopy (OLYMPUS DSX 100) after anodic potentiodynamic polarization tests (see Figure 4). The pitting was evaluated using laser confocal microscopy LEXT OLS 3000 and pitting factor (PF) was calculated according to standard ISO 11463 for all measured steel samples. The calculated pitting factor represents a ratio of the deepest pit to the average depth of 10 measured pits.

Pitting factor of value 1 indicates general corrosion and with the increased value of pitting factor, the pitting corrosion is more prominent.

Tab. 3 *Results of potentiodynamic polarization tests*

	Icorr (μA)	Ecorr (mV)	Rp (Ohm)	CR (mm.a^{-1})	PF (-)
Untreated	2.515	-353.558	15871	0.033	1.21
LTPN	11.856	-412.461	2960	0.153	1.76
LTPN-R	11.081	-464.841	3321	0.143	1.43
HTPN	78.749	-660.211	388	1.019	1.1

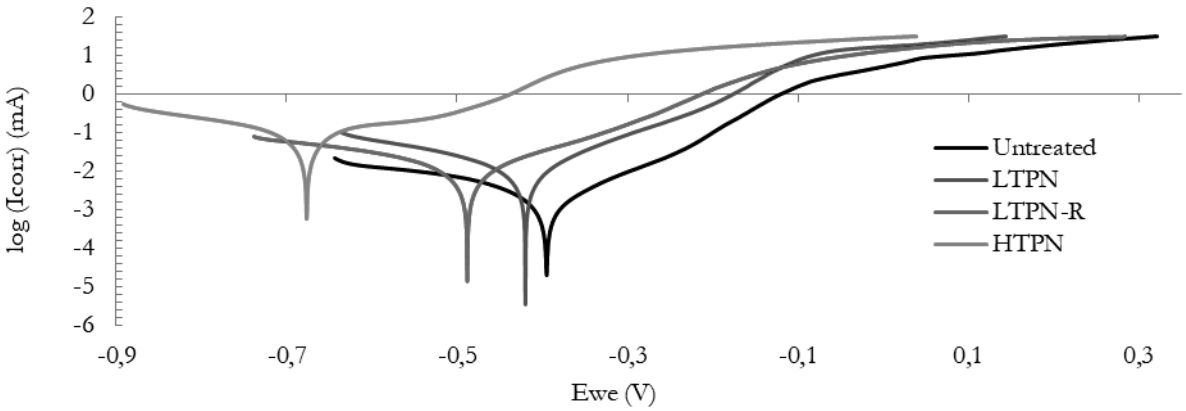

Fig. 6 *PPT measurement in deaerated 2.5% NaCl solution*

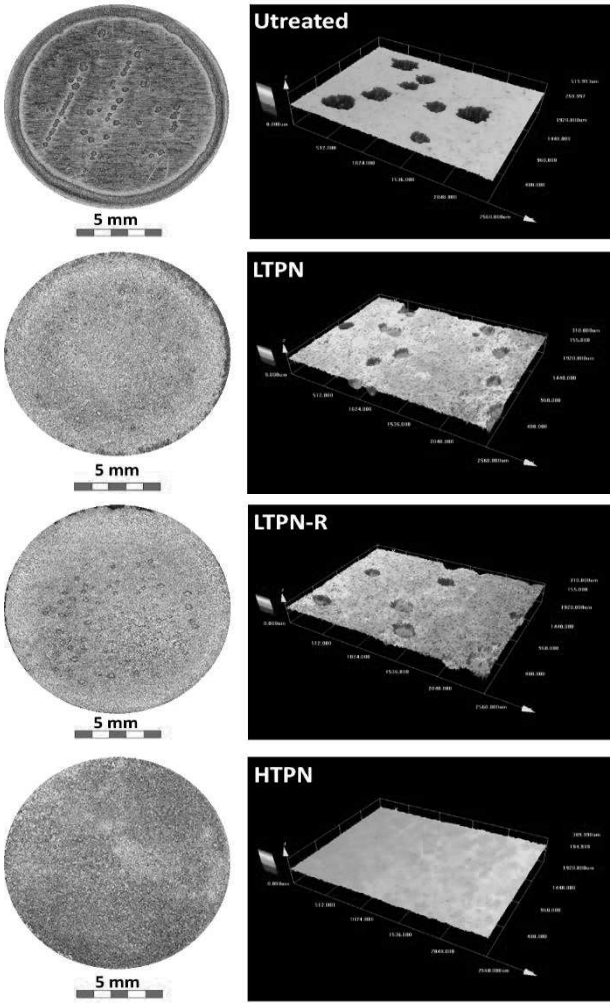

Fig. 7 *2D and 3D surface morphology of the FSS AISI 410 after PTT, 2D on the left (Olympus DSX100), 3D on the right (LEXT OLS 3000)*

The PF calculated for the untreated FSS sample reached the value of PF 1.21 with distinct crevice corrosion under the sealer. The LTPN technique reached a PF value of 1.76, PF = 1.76 for the LTPN-R technique, and PF ~1.1 for the HTPN technique in good agreement with surface documentation in Fig. 7. The maximal depth of pitting (230 μm) was measured on untreated FSS sample, 182 μm for LTPN, and 179 μm for LTPN-R treatment. The HTPN FSS sample was uniformly corroded to an average depth of 24 μm.

3 Conclusion

This paper describes the corrosion resistance of plasma nitrided X12Cr13 ferritic stainless steel (AISI 410) evaluated using the anodic potentiodynamic tests in deaerated 2.5 % NaCl solution compared to the untreated one.

The low-temperature PN techniques (400 °C) increased surface hardness from initial 180-255 HV0.05 to 882 HV0.05 (LTPN), respectively to 1080 HV0.05 (LTPN-R). The high-temperature PN technique increased surface hardness up to 1193 HV0.05 (HTPN). Higher volume of nitrogen in the working atmosphere and higher operational temperature caused higher surface hardness and increased case layer depth.

The initial corrosion rate 0.033 mm·a^{-1} of untreated X12Cr13 steel increased approximately by 5 after low-temperature plasma nitriding up to 0.153 mm·a^{-1} (LTPN), respectively 0.143 mm·a^{-1} (LTPN-R). After high-temperature plasma nitriding (HTPN), the corrosion rate increased approximately by 30 to 1.019 mm·a^{-1}. High-temperature plasma nitriding led to the

highest corrosion rate related to precipitation of Cr_4N_4 and $Cr_{15}Fe_7C_6$ chromium nitrides by depletion of Cr from Cr rich substrate leading to passivation disabling. The HTPN technique applied to the FSS X12Cr13 changed the type of corrosion attack, original pitting to the general type of corrosion with the corresponding value of pitting factor PF ~1.1. According to the calculated pitting factor (PF) can be concluded, the pitting of low-temperature plasma nitrided steel was increased compared to the untreated one.

The presence of Cr_4N_4 and $Cr_{15}Fe_7C_6$ chromium nitrides (CrN) in plasma nitrided X12Cr13 stainless steel indicate reduced chromium content in the solid solution because of Cr_4N_4 and $Cr_{15}Fe_7C_6$ precipitation (HTPN). The Cr depletion led to lower passivation ability after plasma nitriding at 550 °C. Therefore, the HTPN treated X12Cr13 steel tends to the general type of corrosion, corresponding to the more uniformly corroded surface (see Fig. 8).

Summary, plasma nitriding of FSS X12Cr13 at a temperature of 550 °C rapidly deteriorated the corrosion resistance in every aspect compared to the untreated one. But, the surface hardness was greatly increased compared to the untreated one. Can be concluded, that low-temperature nitriding (LTPN and LTPN-R) can achieve the enhanced surface hardness and only slightly increased corrosion rate (reduced corrosion resistance). But the nitride case layer is thinner compared to the high-temperature PN process (HTPN).

Acknowledgment

The present research work was supported by the project The Development of Technologies, Design of Firearms, Ammunition, Instrumentation, Engineering of Materials and Military Infrastructure "VÝZBROJ (DZRO K201)", by specific research programs "Surface technology in applications special techniques SV20-216" and "Materialy a technologie pro elektrotechniku III FEKT-S-17-4595", and CzechNanoLab project LM2018110 by MEYS CR.

References

[1] PYE, D (2003). *Practical nitriding and ferritic nitrocarburizing*. ASM International Materials Park, p. 251 Ohio, USA

[2] POKORNY, Z., DOBROCKY, D., STUDENY, Z. (2018). Influence of Chemical Composition on Layer Properties of Barrel Steels. *Manufacturing Technology*. 18(6), pp. 1007-1010.

[3] ESPITIA, L., A., HANSHAN, D., XIAOYING L., PINEDO, C., E., TSCHIPTSCHIN, A., P. (2017). Scratch test of active screen low temperature plasma nitrided AISI 410 martensitic stainless steel. *Wear*. Vol. 376-377, Part A, Elsevier B.V., pp. 30-36.

[4] ROVANI, A., C., BREGANON, R., GISMAR S. DE SOUZA, G., S., BRUNATTO, S., F., PINTAÚDE, G. (2017). Scratch resistance of low-temperature plasma nitrided and carburized martensitic stainless steel. *Wear*. Vol. 376-377, Part A, Elsevier B.V., pp. 70-76.

[5] DOBROCKY, D., STUDENY, Z., POKORNY, Z., POSPICHAL, M., SMIDA, O. (2016). Effect of plasma nitriding on the notch toughness of spring steel. *METAL 2016. 25th Anniversary International Conference on Metallurgy and Materials*. Tanger Ltd, Ostrava, pp. 1037-1044.

[6] KUSMIC, D., CECH, O., FALTEJSEK, P. (2018). Duplex treatment of plasma nitriding and manganese phosphating of 42CrMo4 steel for corrosion resistance increasing. *METAL 2017, 26th International Conference on Metallurgy and Materials*. TANGER Ltd, Ostrava, pp. 1077-1084.

[7] FALTEJSEK, P., JOSKA, Z., POKORNY, Z., DOBROCKY, D., STUDENY, Z. (2019). Effect of nitriding on the microstructure and mechanical properties of stainless steels. *Manufacturing Technology*. 19(5), pp. 745-748.

[8] NII, H., NISHIMOTO, A. (2012). Surface modification of ferritic stainless steel by active screen plasma nitriding. *Journal of Physics: Conference Series*, Vol 379, IOP Publishing Ltd, p 8.

[9] YANG, W.J., M. ZHANG, Y.H. ZHAO, et al. (2016). Enhancement of mechanical property and corrosion resistance of 316L stainless steels by low temperature arc plasma nitriding. *Surface and Coatings Technology,* Vol. 298, No. C, Elsevier Science, pp. 64-72.

[10] LIANG, W., (2003). Surface modification of AISI 304 austenitic stainless steel by plasma nitriding. *Applied Surface Science*, Vol. 211, Issues 1-4, pp. 308-314.

[11] MENTHE, E., RIE, K.,T. (1999). Further investigation of the structure and properties of austenitic stainless steel after plasma nitriding. *Surface and Coatings Technology*, Vol. 116-119, Elsevier B.V., pp. 199-204.

[12] YANG, Y., WANG, Z., WANG, L. (2014). Surface properties of nitrided layer on AISI 316L austenitic stainless steel produced by high temperature plasma nitriding in short time. *Applied Surface Science*, Vol. 298, Elsevier B.V., pp. 243-250.

[13] LI, C., X., BELL, T. (2006). Corrosion properties of plasma nitrided AISI 410 martensitic stainless steel in 3.5% NaCl and 1% HCl aqueous solutions. *Corrosion Science*, Vol. 48, Issue 8, Elsevier Ltd., pp. 2036-2049.

[14] KUSMIC, D., FALTEJSEK, P. (2019). Corrosion Resistance of Low Temperature Plasma Nitrided X12CrMoWVNbN10-1-1 Martensitic Stainless Steel. *Manufacturing Technology*. Vol. 19, No. 4, pp. 619-623.

[15] CORENGIA, P., YBARRA, G., MOINA, C., CABO, A., BROITMAN, A. (2004). Microstructure and corrosion behaviour of DC-pulsed plasma nitrided AISI 410 martensitic stainless steel. *Surface and Coatings Technology*, Vol. 187, Issue 1, Elsevier B.V., pp. 63-69.

[16] PINEDO, C. E., VARELA, L. B., TSCHIPTSCHIN, A. P. (2013). Low-temperature plasma nitriding of AISI F51 duplex stainless steel. *Surface & Coatings Technology*, Vol. 232, Elsevier Science, pp. 839-843.

[17] MIYAMOTO, G., YONEMOTO, A., TANAKA, Y., FURUHARA, T., MAKI, T. (2006). Microstructure in a plasma-nitrided Fe-18 mass% Cr alloy. *Acta Materialia*, Vol. 54, pp. 4771-4779.

[18] BORGIOLI, F.,FOSSATI, A., GALVANETTO, E., BACCI, T. (2005). *Surface & Coatings Technology,* Vol. 200, pp. 2477-2480.

[19] TSUJIKAWA, M., YAMAUCHI, N., UEDA, N., SONE, N., HIROSE, Y. (2005). Behavior of carbon in low temperature plasma nitriding layer of austenitic stainless steel. *Surface and Coatings technology,* Vol. 193(1), pp. 309-313.